Journal of Applied Physics

Photogating and high gain in ReS_2 field-effect transistors

Cite as: J. Appl. Phys. **124**, 204306 (2018); https://doi.org/10.1063/1.5050821
Submitted: 02 August 2018 . Accepted: 02 November 2018 . Published Online: 29 November 2018

C. Garcia, N. R. Pradhan, D. Rhodes, L. Balicas, and S. A. McGill

COLLECTIONS

This paper was selected as an Editor's Pick

View Online Export Citation CrossMark

ARTICLES YOU MAY BE INTERESTED IN

Analog high resistance bilayer RRAM device for hardware acceleration of neuromorphic computation
Journal of Applied Physics **124**, 202101 (2018); https://doi.org/10.1063/1.5042432

Effect of stacking faults and surface roughness on the thermal conductivity of InAs nanowires
Journal of Applied Physics **124**, 205101 (2018); https://doi.org/10.1063/1.5051677

Tuning the band alignment of p-type graphene-AsSb Schottky contact by electric field
Journal of Applied Physics **124**, 204301 (2018); https://doi.org/10.1063/1.5054614

© 2018 Author(s).

Photogating and high gain in ReS_2 field-effect transistors

C. Garcia,[1,2] N. R. Pradhan,[2,3,a)] D. Rhodes,[1,2,b)] L. Balicas,[2] and S. A. McGill[2,a)]
[1]*Physics Department, Florida State University, 77 Chieftan Way, Tallahassee, Florida 32306, USA*
[2]*National High Magnetic Field Laboratory, 1800 E. Paul Dirac Dr., Tallahassee, Florida 32310, USA*
[3]*Department of Chemistry, Physics and Atmospheric Science, Jackson State University, 1400 John R. Lynch St, Jackson, Mississippi 39217, USA*

(Received 2 August 2018; accepted 2 November 2018; published online 29 November 2018)

Two-dimensional layered transition metal dichalcogenides have shown much promise due to their remarkable electro-optical properties and potential use as photodetectors. We observed photogating in our few-layered (3–4 layers) ReS_2 field-effect transistors (FETs) in which varying the incident optical power shifted the FETs' threshold voltage. The photogating effect produced a significant gain in the electrical response of the FETs to incident light as measured by the responsivity (R) and external quantum efficiency (EQE). We obtained a maximum R of 45 A/W corresponding to an EQE of ~10 500% in a four-terminal measurement of the photoconductivity in the ON-state. We attribute both the photogating and the observed gain to the influence of charge traps. An estimate of the device gain based on our observations is calculated to be 5×10^4. *Published by AIP Publishing.*
https://doi.org/10.1063/1.5050821

I. INTRODUCTION

Two-dimensional materials, particularly transition metal dichalcogenides (TMDs), have caught much attention due to their interesting properties. For instance, they are known to have sizable carrier mobility and high optical transparency while retaining strong interactions with light and tunable bandgaps.[1,2] Certain TMDs, such as molybdenum disulphide (MoS_2), are noted for their natural availability, optical and electrical properties, and their bandgap tunability from indirect gap to direct gap.[3] In single layer form, MoS_2 shows mobility as high as 55 $cm^2\,V^{-1}\,s^{-1}$ with a large ON/OFF current ratio of 10^8.[4–6] There also has been a report of WSe_2 having a mobility of 110 $cm^2\,V^{-1}\,s^{-1}$.[7] Recent reports on monolayer MoS_2 show that the responsivity can range from a few mA/W to hundreds of A/W.[6,8]

ReS_2, alternatively, is predicted to be a direct bandgap material,[9,10] where the bandgap does not depend upon the number of layers unlike other TMDs such as MoS_2, $MoSe_2$, WSe_2, etc., thus making it a potential candidate for optoelectronic applications. ReS_2 has a unique distorted 1*T* crystal structure, unlike many TMDs with a 2*H* crystal phase, which exhibits unique in-plane anisotropic transport properties further making it a promising candidate for logic circuits.[11] Therefore, it is important to study the optical properties of this material to explore its potential for optoelectronic applications. ReS_2 has shown great promise as a semiconductor for field-effect transistors (FETs) and is still improving in performance.[12] Responsivity in multi-layer ReS_2-FETs (up to 30 nm thick) has been reported as high as 2.5×10^7 A/W.[13,14] In this paper, we report our observations of photogating in few-layered (3–4 layers) ReS_2-FETs and discuss how it is coupled with material defects and device gain. We also report the responsivity and external quantum efficiency in two- and four-terminal measurement configurations. To the best of our knowledge, our report is the first discussion of photogating and its effects in ReS_2-based FETs.

Figure 1(a) shows a schematic of a ReS_2-FET on the SiO_2/Si substrate along with the measurement strategy. The typical channel length and average width were $L = 12.5\,\mu$m and $W = 3.5\,\mu$m, respectively. The photoconductivity measurements were performed in a home-built microscope equipped with a 532 nm laser source. Further details of the optical setup for this experiment can be found in a previous report.[15] The laser was unpolarized and the spot size was 30–35 μm, which was larger than the device. The spot size was measured using the lithographically patterned grids on the Si wafer in order to calculate the incident optical fluence. Figure 1(b) is a micrograph of the ReS_2 device that has five contacts, enabling both 2-terminal and 4-terminal measurements. In 4-terminal measurements, two voltage leads (V+ and V−) and two current leads (I+ and I−) were implemented to measure the intrinsic photoconductivity of the ReS_2. In the 2-terminal measurements, only the (I+ and I−) contacts were used. The FET and photoconductivity properties were measured using a Keithley 2400 and 2612A. The back-gate voltage (V_{bg}) was used to modulate the carrier population in the ReS_2. All of the measurements were conducted under ambient conditions and in a dark-room environment. The data collection was automated using LabVIEW-based custom software.

II. MATERIALS AND DEVICE SYNTHESIS

ReS_2 single crystals were synthesized through a chemical vapor transport technique using either iodine or excess sulfur as the transport agent. The synthesis technique of the ReS_2 crystal process is described in a prior report.[16] The quality of these ReS_2 single crystals was checked by EDX and Raman spectroscopy.[16] Multi-layered flakes of ReS_2

a)Authors to whom correspondence should be addressed: mcgill@magnet.fsu.edu and nihar.r.pradhan@jsums.edu
b)Current address: Center for Integrated Science and Engineering, Columbia University, New York, New York 10027, USA

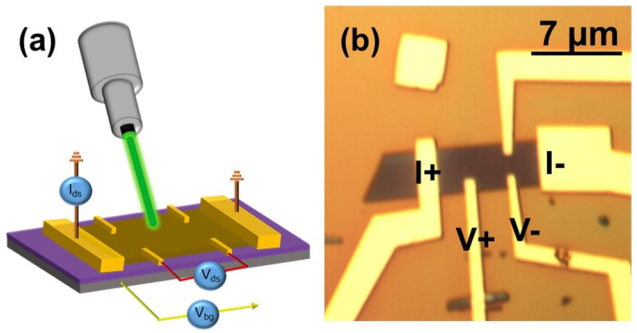

FIG. 1. (a) Illustration of a ReS_2-FET on a Si/SiO_2 substrate with laser illumination. Drain-source excitation is applied as shown on the sample with a back-gate voltage terminal under the SiO_2 dielectric layer. 532 nm laser illumination is applied to the sample and varied with an optical attenuator. (b) The optical image of a four-terminal transistor that is fabricated on a SiO_2 substrate grown on top of highly p-doped Si.

were exfoliated from these single crystals using the micromechanical cleavage technique. These exfoliated thin layers of ReS_2 were then transferred onto a clean 278 nm thick SiO_2 substrate grown on a degeneratively p-doped Si wafer and identified under an optical microscope. The thickness of the flakes was determined via atomic force microscopy. We used standard electron-beam lithography techniques to pattern the contacts, and then an electron beam evaporator at 10^{-7} Torr to deposit the Cr/Au (~4/90 nm) contacts. The FETs were annealed at 350 °C for 3 h in forming gas, followed by vacuum (10^{-7} Torr) annealing at 130 °C for 24 h.

III. RESULTS AND DISCUSSION

We first measured the electrical performance of the ReS_2-FETs in the dark using both 2-terminal and 4-terminal methods to investigate the influence of the contact resistance. Figure 2(a) shows the two-terminal source-drain current (I_{ds}) without laser illumination as a function of drain-source voltage (V_{ds}) under multiple back-gate voltages. Figure 2(b) shows the equivalent transport measurements but in the 4-terminal configuration. The two configurations exhibited a linear response for the range of V_{ds} and V_{bg} we applied. This is characteristic of thermionic emission of carriers that allows them to pass the Schottky barrier between the Cr/Au contact and the ReS_2 crystal.[15] In n-type conduction, a positive back-gate voltage increases the number of charge carriers in the device thereby increasing the measured current in both configurations. For $V_{bg} = 40$ V in the 2-terminal geometry, the maximum current was 236 nA at $V_{ds} = 150$ mV. This increased by about a factor of three to 856 nA in 4-terminal geometry [Fig. 2(b)] thereby making the 4-terminal ON/OFF ratio ~10^4.

By varying V_{bg}, as shown in Figs. 2(c) and 2(d), we compared the electrical transport properties of the device for both measurement configurations with no illumination. We limited the power dissipation in the devices in order to prevent damage by applying a small drain-source voltage. The increase in current for positive V_{bg} again demonstrated the n-type conduction in these FETs. For $V_{ds} = 150$ mV and $V_{bg} = 50$ V, the maximum 2-terminal current was 343 nA, while it was at least three times larger in the 4-terminal configuration at 1252 nA. These differences can be attributed to the reduction in the effects of contact resistance present in the 2-terminal configuration. Therefore, the 4-terminal technique provided a more accurate measurement of the intrinsic charge mobility through the ReS_2.[17] The 2-terminal field-effect electron mobility can be calculated using[15]

$$\mu_{fe-2t} = \frac{dI_{ds}}{dV_{bg}} \times \frac{L}{WV_{ds}C_i}, \tag{1}$$

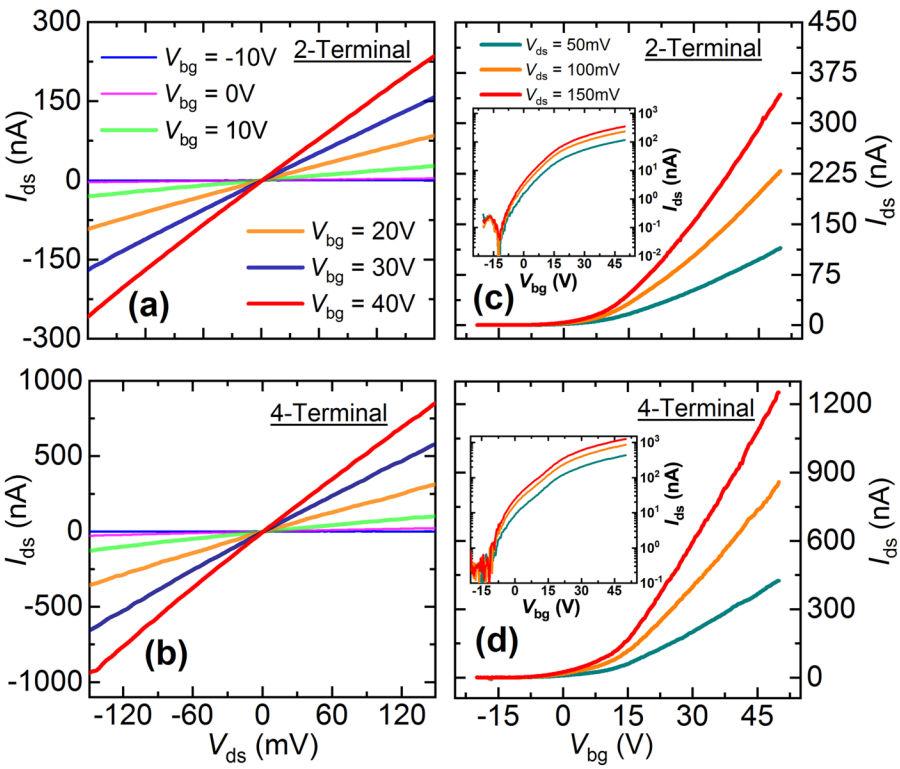

FIG. 2. Comparison between the transport properties of few-layered ReS_2-FETs when measured in 2- and 4-terminal configurations with no laser illumination. (a) and (b) Drain-source current (I_{ds}) as a function of the drain-source voltage (V_{ds}) in 2- and 4-terminal configurations, respectively. Several back-gate voltages ranging from −10 to 40 V were used. (c) and (d) I_{ds} as a function of the applied back-gate voltage, V_{bg}, for 2- and 4-terminal configurations for several drain-source voltages. The insets show the same data on a semi-logarithmic scale.

where dI_{ds}/dV_{bg} is the linear slope, $C_i = \epsilon\epsilon_0/d = 11.783 \times 10^{-9}$ F cm^{-2} is the gate capacitance per unit area, $\epsilon(=3.9)$ is the dielectric constant of SiO_2, d is the thickness of the gate dielectric, L (=12.5 μm) is the channel length, and W (=3.5 μm) is the width of the channel. The 2-terminal field-effect mobility was 18.7 cm^2 V^{-1} s^{-1}. The 4-terminal field-effect mobility was calculated using[16]

$$\mu_{fe-4t} = \frac{l_v}{WC_i} \times \frac{d[(I_{ds} - I_0)/V_{12}]}{dV_{bg}}, \tag{2}$$

where l_v is the length between the two voltage leads, I_0 is the OFF-current, and V_{12} is the voltage measured between the voltage leads. Using this equation, the 4-terminal mobility was 20.2 cm^{2}V^{-1}s^{-1}.

Our initial photoconductivity measurements compared the responsivity (R) and external quantum efficiency (EQE) of the devices in 2- and 4-terminal configurations. The responsivity was defined as $R = I_{ph}/P_{opt}$, where I_{ph} is the photocurrent and P_{opt} is the incident optical power. The photocurrent, $I_{ph} = I_{light} - I_{dark}$, was calculated by subtracting the dark current, I_{dark}, from the measured current when laser illumination was applied. P_{opt} was found using $P_{opt} = \frac{P}{\pi r^2} \times A$, where P is the actual laser output, A is the area of the sample, and r is the radius of the laser spot size. In our measurements, the incident laser power on the sample ranged from 10 nW to 10 μW. We varied the optical power while V_{ds} and V_{bg} were held constant. The values for V_{ds} ranged from 100 mV to 500 mV for V_{bg} at 10 V. Figures 3(a) and 3(b) show R as a function of the incident optical power P_{opt} using 2- and 4-terminal configurations, respectively. The responsivity was at the largest when P_{opt} was low, at ~10 nW. The 2-terminal responsivity was 16 A/W for $V_{ds} = 500$ mV and $V_{bg} = 10$ V. For the same V_{ds} and V_{bg}, the 4-terminal responsivity was 45 A/W, about three times larger.

The responsivity extracted from our few-layered ReS_2 device was much smaller than the responsivity reported on a single-layer MoS_2 phototransistor[6] (i.e., 880 A/W). But this responsivity of single-layer MoS_2 was measured at an incident power of 150 pW and applied $V_{ds} = 8$ V. The responsivity measured in our ReS_2 device was 45 A/W under an incident power of 13 nW and an applied $V_{ds} = 0.5$ V. If we compare these values with those from a single-layer MoS_2 device, its responsivity at a 10 nW incident power is 100 A/W but at much higher drain-source voltage. Our previous investigation[15] suggested that the responsivity scales up with the applied V_{ds}. Thus, the responsivity on the few-layered ReS_2-FET is comparable to that of the MoS_2 device.

In Fig. 3(b), we fitted R to P_{opt} using a power law, $P_{opt}^{-\gamma}$. The extracted value of gamma from the fitting was $\gamma = 0.90$. The sublinear dependence is thought to be caused by the presence of charge traps which can occur on the surface of ReS_2, in the gate dielectric, or at the interface between ReS_2 and the SiO_2 layer.[6,18] The influence of charge traps in ReS_2 could be particularly significant due to the large surface-to-volume ratio of these few-layered ReS_2 samples and may help to account for the large responsivities observed.[19] Photoexcitation may either populate charge into traps or liberate charge from traps leading to an increase in I_{ds} in the OFF-state and sub-linear

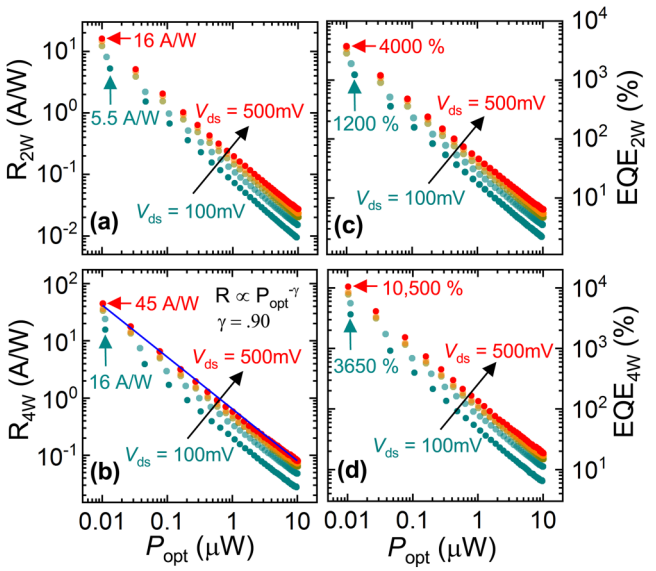

FIG. 3. (a) and (b) Logarithmic plots of the responsivity for a few-layered ReS_2-FET as a function of the illumination power for a 2- and a 4-terminal configuration, respectively. (c) and (d) EQE values extracted using (3). $V_{bg} = 10$ V for all data in this figure. Both R and EQE were plotted for a range of applied V_{ds}, from 100 mV to 500 mV. The blue solid line in (b) is a linear fit to R as a function of P_{opt} taken with $V_{ds} = 500$ mV to extract the exponent γ. R_{2W} and EQE_{2W} correspond to R and EQE measured with a 2-terminal configuration while R_{4W} and EQE_{4W} correspond to the 4-terminal configuration.

threshold regions of the device, at least for the lifetime of the photoinduced response. This effect would decrease as the incident optical intensity increases, producing smaller responsivities and finally saturating.[19]

In addition to R, we calculated the EQE. The EQE is the ratio of the number of photoexcited charge carriers to the number of incident photons

$$\mathrm{EQE} = \frac{hc(\mathrm{R})}{\lambda e}, \tag{3}$$

where R is the responsivity, λ is the excitation wavelength, and e is the electron charge. The EQE is plotted as a function of P_{opt} in both 2- and 4-terminal configurations in Figs. 3(c) and 3(d), respectively. For the 2-terminal configuration, the EQE at $P_{opt} = 13$ nW and $V_{ds} = 100$ mV is ~1200% but at 10 nW when $V_{ds} = 500$ mV, the value rose to ~4000%. This clearly indicates that as V_{ds} increases, the EQE rises as well. This also holds true with the 4-terminal configuration. At $P_{opt} = 11$ nW and $V_{ds} = 100$ mV, the EQE is ~3650% and for P_{opt} at 10 nW and $V_{ds} = 500$ mV, the EQE jumps to ~10 500%. This is larger in comparison to the 2-terminal EQE value (i.e., larger by a factor of ~3). Previous reports showed that in a 2-terminal ReS_2-FET, the responsivity and EQE values were 16.14 A/W and 3168%, respectively.[12] The combination of the sublinear dependence of R on P_{opt} and the high R and EQE values suggest the presence of a charge trap-mediated gain mechanism. In this scenario, photoexcitation initially populates or depopulates the charge traps, producing the sublinear dependence on P_{opt}. Gain occurs if the lifetime of the photoexcited charge exceeds the transit time of charge carriers.

Other TMDs, such as MoS_2 and WSe_2, have demonstrated multiple photocurrent generation mechanisms.[20,21] These mechanisms include the photoconductive, photoelectric, photothermoelectric, and photovoltaic effects. In certain operating conditions, some of these or all may affect the sample and alter the device's response time and photoconductivity. In our ReS_2-FETs, we observed a photogating effect and did not observe a photothermoelectric effect.[22] We measured multiple samples that displayed photogating, but the amount of threshold shift was sample dependent. Figure 4(a) shows the drain-source current as a function of the back-gate voltage in the 4-terminal configuration. As laser illumination (532 nm) ranging from 0 to 1.2 μW was applied to the sample with $V_{ds} = 100$ mV, the threshold voltage from Fig. 4(a) shifted to the left. This leftward shift of the voltage threshold (V_{th}) increased with laser intensity and saturated. The voltage threshold is plotted in Fig. 4(b). The trapped charge density was also plotted as a function of P_{opt} in Fig. 4(b). This charge density was estimated using $n = e^{-1}C_i|\Delta V_{th}|$, where C_i is the gate capacitance per unit area and ΔV_{th} is the shift in the threshold voltage caused by illumination.[23] The density of trapped charges increased with the incident optical power but saturated at about 9×10^{11} cm^{-2}.

The decrease in R and EQE are likely a consequence of photoinduced effects on charge traps in ReS_2. It has been reported that sulfur vacancies produce deep donor defect states in MoS_2.[24] If similar donor states exist in our ReS_2, it is possible that photoexcitation initially liberates these trapped charges leading to a large R and EQE, which is then diminished with increasing incident laser fluence as traps are depopulated. An alternate explanation is that increased photoexcitation reduces available charge due to the creation of more traps filled with photocarriers.[12] Traps likely also explain the photogating and gain phenomena as well. Photoexcitation produces electrons and holes, which are pulled toward the electrodes of the device due to the applied V_{ds}. If the mobility of holes is significantly smaller than that of electrons, it is possible that many more electrons will participate in photoconduction than holes thereby producing gain.[2] The observation of photogating suggests that a layer of additional positive charge is photoinduced at the interface between ReS_2 and SiO_2 and contributes to gating the channel. If this additional positive charge is produced by the photoexcitation of ReS_2 and is trapped, the electron-hole recombination time may be further prolonged and thus additionally enhance the gain.

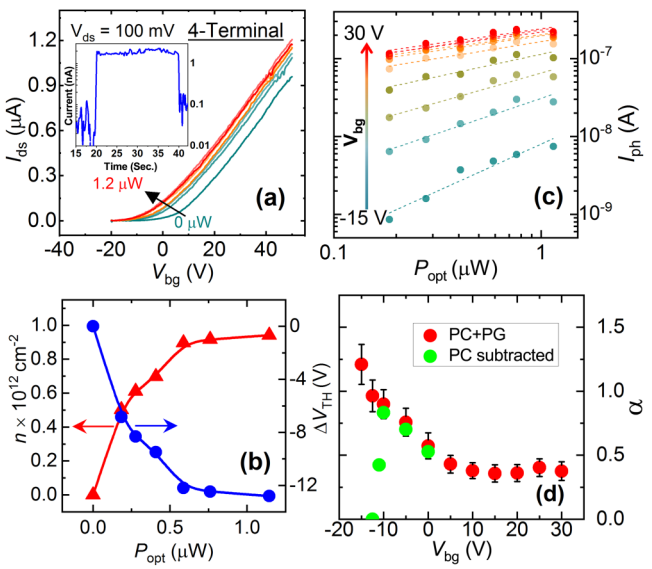

FIG. 4. (a) Source-drain current as a function of back-gate voltage. The laser power was varied from 0 to 1.2 μW. The inset shows the switching performance, measured on an alternate device, at $V_{bg} = 0$ V and $V_{ds} = 100$ mV. (b) The estimated trapped charge density (triangles) and the shift of the threshold voltage (circles) as a function of P_{opt}. (c) Photocurrent, I_{ph}, as a function of P_{opt}, where V_{bg} was varied from −15 to 30 V. The dotted lines show the power law fit $I_{ph} \propto P_{opt}^{\alpha}$. (d) α as a function of V_{bg}. Red circles denote α for the total photocurrent and green circles denote α for photogating contribution of the photocurrent with linear photoconduction background removed. For $V_{bg} > 0$, the red and green circles overlap each other. Error bars represent the standard error of the linear fits from panel (c) for the total photocurrent.

The photoconduction mechanism is defined by the linear response of I_{ph} to the incident optical power.[20] When this relationship becomes sublinear, the mechanism is referred to as photogating.[25,26] The interplay of these two phenomena in our devices can be examined by plotting the current as a function of optical power, as in Fig. 4(c). As this relationship is plotted for various V_{bg} and analyzed with a power law, $I_{ph} \propto P_{opt}^{\alpha}$, α takes on a continuous range of values but is sublinear for $V_{bg} > -12$ V. This figure shows that the FET can be tuned from fast photoconduction in the OFF-state to high gain photogating in the ON-state.[20] The results of the power law fitting are shown in Fig. 4(d). In the OFF-state at $V_{bg} \leq -12$ V, $\alpha = 1$ and we observed photoconduction, which accounted for photoinduced current on the order of 10^{-8} A. In order to differentiate this linear increase in the photocurrent from the effects of photogating, we replotted α after subtracting this linear photoconduction response as a background from the total photocurrent at higher V_{bg}. Essentially, we estimated the total photocurrent as a sum of the linear photoconductive response defined by the curve for $\alpha = 1$ in Fig. 4(c) and a sub-linear photogating response. After removing this linear response, the onset and peak of the photogating mechanism with V_{bg} became clearer. The contribution of the photogating effect rapidly became the dominant contribution to the total photoinduced current for $V_{bg} \geq -10$ V. The peak α for the photogating contribution was $\alpha \sim 0.8$. Though α decreased throughout the sublinear threshold region as photoinduced effects saturated,[7] significant gain was still maintained into the ON-state, as observed in Fig. 3.

An estimate of the gain due to photogating, based on a trap-mediated mechanism, can be calculated by using Gain $= \tau_{photo}/\tau_{transit}$, where τ_{photo} is the average lifetime of the photoexcited charge carrier and $\tau_{transit}$ is the transit time of a charge carrier through the channel.[2,3] The transit time can be rewritten as $\tau_{transit} = L^2/\mu_{fe-4t}V_{ds} = 774$ ns, where L is the channel length (= 12.5 μm), μ_{fe-4t} is the field-effect electron mobility (= 20.2 cm^{2}V^{-1}s^{-1}), and V_{ds} is the drain-source voltage (= 100 mV). We estimated the photoexcited charge lifetime using a measurement of the switching speed of the device back to the dark state current once the photoexcitation was removed. This lifetime in our devices was about 40 ms, which is consistent with similar reports involving semiconductor charge traps in other studies.[7,20,27,28] The switching

behavior is shown in Fig. 4(a) inset on an alternate device. Our light source was switched by a mechanical shutter with a speed of ≤ 20 ms and the device switched off and on faster than our data sampling rate (~ 10 Hz). The decay time of the photocurrent is an estimate based on the assumption of a single exponential decay of the photocurrent within the measured decay period (2-terminal configuration). We note this since significantly faster switching times (e.g., $7.5\,\mu$s)[29] in other two-dimensional systems have been reported. Therefore, it is possible that the actual charge lifetimes in ReS_2 could be significantly shorter. Using our calculation, we estimated the gain at 5×10^4, which is orders of magnitude bigger when compared to the EQE. This could be partially due to the low absorption one expects in a sample only a few atomic layers thick. The EQE value represents a lower bound of the gain due to less than perfect absorption.

In order to quantify the ultimate sensitivity of our devices to incident light, we estimated the noise equivalent power (NEP) of the FET used as a photodetector. For the case in which the noise is limited to the shot noise of the dark current, we calculated the shot noise to be about 17 fA for the dark current at $V_{bg} = -10$ V. Under the assumption that the responsivity of the device is maintained below the minimum incident optical power we applied of 10 nW, the minimum incident power to increase the current above the noise level can be calculated using the power law relationship obtained in the discussion of Fig. 4(c). The NEP of the device within these parameters is $\sim$1 fW. This is equivalent to an incident flux of $\sim 10^3 - 10^4$ photons/s. The actual noise we encountered in our measurements was significantly larger than this limiting case.

IV. CONCLUSION

In summary, we characterized the few-layered ReS_2-FETs in dark conditions and under laser illumination. We contrasted the phototransport properties both in the conventional 2-terminal and 4-terminal configurations. We calculated and analyzed the responsivity and the external quantum efficiency as functions of the incident optical power in both configurations. Our investigation showed that the 4-terminal configuration provided higher values for both the responsivity and the external quantum efficiency due, at least in part, to the reduced effects of the contact resistance. We also showed that photocurrent generation occurred in the device and had significant effects on the phototransport measurements in the OFF-state. It was also shown that the device had a photoresponse which resembled fast photoconduction in the OFF-state while switching to a high photogating gain in the ON-state. The photogating effect was estimated to be able to produce a 5×10^4 gain, based on the assumption that the source of the gain was the interaction of photoinduced charge with trap states either in ReS_2, the gate dielectric, or the interface between the two. This estimate was two orders of magnitude higher than the measured EQE. In the future, it would be interesting to do a more detailed electronic spectroscopy of the subthreshold region which includes the energy range of the charge traps. This would require a device construction that makes it possible to compare the gate potential and the Fermi energy within the channel. ReS_2 and other materials like it may have a promising future in photovoltaic and other optoelectronic-based applications.

ACKNOWLEDGMENTS

The authors wish to acknowledge funding for this research from the National Science Foundation via DMR-1229217. L.B. acknowledges support from the US Army Research Office through the MURI Grant No. W911NF-11-10362 and NSF through DMR-1807969. A portion of this work was performed at the National High Magnetic Field Laboratory, which is supported by the National Science Foundation Cooperative Agreements DMR-1157490 and DMR-1644779 and the State of Florida.

[1]A. Splendiani, L. Sun, Y. Zhang, T. Li, J. Kim, C.-Y. Chim, G. Galli, and F. Wang, Nano Lett. **10**, 1271 (2010).
[2]M. Buscema, J. O. Island, D. J. Groenendijk, S. I. Blanter, G. A. Steele, H. S. J. van der Zant, and A. Castellanos-Gomez, Chem. Soc. Rev. **44**, 3691 (2015).
[3]X. Liu, T. Galfsky, Z. Sun, F. Xia, E.-c. Lin, Y.-H. Lee, S. Kna-Cohen, and V. M. Menon, Nat. Photon **9**, 30 (2015).
[4]B. Radisavljevic, A. Radenovic, J. Brivio, V. Giacometti, and A. Kis, Nat. Nanotechnol. **6**, 147 (2011).
[5]M. S. Fuhrer and J. Hone, Nat. Nanotechnol. **8**, 146 (2013).
[6]O. Lopez-Sanchez, D. Lembke, M. Kayci, A. Radenovic, and A. Kis, Nat. Nanotechnol. **8**, 497 (2013).
[7]C. Hu, D. Dong, X. Yang, K. Qiao, D. Yang, H. Deng, S. Yuan, J. Khan, Y. Lan, H. Song, and J. Tang, Adv. Funct. Mater. **27**, 1603605 (2017).
[8]Z. Yin, H. Li, H. Li, L. Jiang, Y. Shi, Y. Sun, G. Lu, Q. Zhang, X. Chen, and H. Zhang, ACS Nano **6**, 74 (2012).
[9]S. Tongay, H. Sahin, C. Ko, A. Luce, W. Fan, K. Liu, J. Zhou, Y.-S. Huang, C.-H. Ho, J. Yan, D. F. Ogletree, S. Aloni, J. Ji, S. Li, J. Li, F. M. Peeters, and J. Wu, Nat. Commun. **5**, 3252 (2014).
[10]S. Horzum, D. Çakır, J. Suh, S. Tongay, Y.-S. Huang, C.-H. Ho, J. Wu, H. Sahin, and F. M. Peeters, Phys. Rev. B **89**, 155433 (2014).
[11]E. Liu, Y. Fu, Y. Wang, Y. Feng, H. Liu, X. Wan, W. Zhou, B. Wang, L. Shao, C.-H. Ho, Y.-S. Huang, Z. Cao, L. Wang, A. Li, J. Zeng, F. Song, X. Wang, Y. Shi, H. Yuan, H. Y. Hwang, Y. Cui, F. Miao, and D. Xing, Nat. Commun. **6**, 6991 (2015).
[12]E. Zhang, Y. Jin, X. Yuan, W. Wang, C. Zhang, L. Tang, S. Liu, P. Zhou, W. Hu, and F. Xiu, Adv. Funct. Mater. **25**, 4076 (2015).
[13]E. Liu, M. Long, J. Zeng, W. Luo, Y. Wang, Y. Pan, W. Zhou, B. Wang, W. Hu, Z. Ni, Y. You, X. Zhang, S. Qin, Y. Shi, K. Watanabe, T. Taniguchi, H. Yuan, H. Y. Hwang, Y. Cui, F. Miao, and D. Xing, Adv. Funct. Mater. **26**, 1938 (2016).
[14]J. Shim, A. Oh, D.-H. Kang, S. Oh, S. K. Jang, J. Jeon, M. H. Jeon, M. Kim, C. Choi, J. Lee, S. Lee, G. Y. Yeom, Y. J. Song, and J.-H. Park, Adv. Mater. **28**, 6985 (2016).
[15]N. R. Pradhan, C. Garcia, J. Holleman, D. Rhodes, C. Parker, S. Talapatra, M. Terrones, L. Balicas, and S. A. McGill, 2D Mater. **3**, 041004 (2016).
[16]N. R. Pradhan, A. McCreary, D. Rhodes, Z. Lu, S. Feng, E. Manousakis, D. Smirnov, R. Namburu, M. Dubey, A. R. Hight Walker, H. Terrones, M. Terrones, V. Dobrosavljevic, and L. Balicas, Nano Lett. **15**, 8377 (2015).
[17]N. R. Pradhan, D. Rhodes, Q. Zhang, S. Talapatra, M. Terrones, P. M. Ajayan, and L. Balicas, Appl. Phys. Lett. **102**, 123105 (2013).
[18]S. Ghatak, A. N. Pal, and A. Ghosh, ACS Nano **5**, 7707 (2011).
[19]S. R. Tamalampudi, Y.-Y. Lu, U. R. Kumar, R. Sankar, C.-D. Liao, B. K. Moorthy, C.-H. Cheng, F. C. Chou, and Y.-T. Chen, Nano Lett. **14**, 2800 (2014).
[20]J. O. Island, S. I. Blanter, M. Buscema, H. S. J. van der Zant, and A. Castellanos-Gomez, Nano Lett. **15**, 7853 (2015).
[21]M. Yamamoto, K. Ueno, and K. Tsukagoshi, Appl. Phys. Lett. **112**, 181902 (2018).
[22]N. Perea-Lòpez, Z. Lin, N. R. Pradhan, A. Iñiguez-Rábago, A. L. Elas, A. McCreary, J. Lou, P. M. Ajayan, H. Terrones, L. Balicas, and M. Terrones, 2D Mater. **1**, 011004 (2014).
[23]C.-H. Lee, G.-H. Lee, A. M. van der Zande, W. Chen, Y. Li, M. Han, X. Cui, G. Arefe, C. Nuckolls, T. F. Heinz, J. Guo, J. Hone, and P. Kim, Nat. Nanotechnol. **9**, 676 (2014).

[24]H. Qiu, T. Xu, Z. Wang, W. Ren, H. Nan, Z. Ni, Q. Chen, S. Yuan, F. Miao, F. Song, G. Long, Y. Shi, L. Sun, J. Wang, and X. Wang, Nat. Commun. **4**, 2642 (2013).
[25]H.-S. Kang, C.-S. Choi, W.-Y. Choi, D.-H. Kim, and K.-S. Seo, Appl. Phys. Lett. **84**, 3780 (2004).
[26]Y. Takanashi, K. Takahata, and Y. Muramoto, IEEE Trans. Electron Dev. **46**, 2271 (1999).
[27]G. Konstantatos, M. Badioli, L. Gaudreau, J. Osmond, M. Bernechea, F. P. G. de Arquer, F. Gatti, and F. H. L. Koppens, Nat. Nanotechnol. **7**, 363 (2012).
[28]Y. Liu, F. Wang, X. Wang, X. Wang, E. Flahaut, X. Liu, Y. Li, X. Wang, Y. Xu, Y. Shi, and R. Zhang, Nat. Commun. **6**, 8589 (2015).
[29]S. Ghosh, P. D. Patil, M. Wasala, S. Lei, A. Nolander, P. Sivakumar, R. Vajtai, P. Ajayan, and S. Talapatra, 2D Mater. **5**, 015001 (2017).